

## 13.6 Numerical simulations of tornado-producing supercell storm and tornado associated with Typhoon Shanshan (2006)

Wataru Mashiko

Meteorological Research Institute, JMA, 1-1 Nagamine, Tsukuba, Ibaraki 305-0052, Japan  
(e-mail : [wmashiko@mri-jma.go.jp](mailto:wmashiko@mri-jma.go.jp))

### 1. Introduction

On 17 September 2006, three tornados hit the Miyazaki Prefecture, western Japan, during the passage of the rainband that accompanied Typhoon Shanshan (2006). The tornado which hit Nobeoka city caused most severe damage with a F-2 scale. In order to reveal the environmental fields and the storms which spawned the tornados, the numerical simulations were conducted. Moreover, the super-high-resolution simulation with the horizontal grid spacing of 50 m was attempted to reproduce the tornado itself.

### 2. Overview of synoptic and mesoscale fields based on observational data

Strong typhoon Shanshan with a central pressure of 950 hPa moved north-northeastward at a speed of  $35 \text{ km h}^{-1}$  over the ocean in the west of Kyusyu Island when three tornados hit Nichinan, Hyuuga and Nobeoka city in Miyazaki prefecture at about 1210, 1330 and 1400 JST respectively (Fig. 1). The occurrence point of each tornado is located in the right-front quadrant of the translating typhoon.

Radar image shows that two adjacent rainbands extended from the north to the east side of the typhoon about 300 km away from the storm center (Fig. 2). All of three tornados were generated during the passage of the outer one, which consists of a number of isolated active convective cells with a horizontal scale of 20 – 40 km (Fig. 3a and 3b). Some of them lasted for more than 2 hours and spawned the tornados.

Nobeoka tornado caused most severe damage and killed 3 persons. A detailed damage survey revealed the following points: (1) the

tornado moved north-northwestward at a speed of about  $90 \text{ km h}^{-1}$  from 1403 to 1408 JST (JST = UTC + 9 hours); (2) damage swath was 7.5 km in length and 150 - 300 m in width; (3) the tornado was ranked as F-2 on the Fujita scale.

A pressure drop of about 1 hPa was recorded at Nobeoka meteorological observatory, about 1000 m west of the tornado path. However, this pressure drop is not considered to be caused by the tornado because the location of the observatory was far from the tornado path and about 7-min duration of the pressure drop was too long. Therefore, it can be inferred that the pressure decrease was caused by the parent-storm which spawned the tornado. As to the surface temperature field, the gradual and weak temperature decrease about 1 - 2 K was observed during the passage of the isolated convective cells.

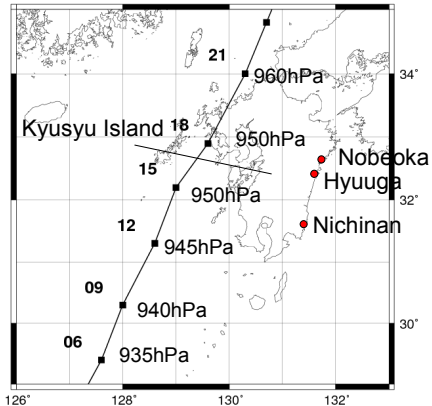


Fig. 1. The best track analysis of Typhoon Shanshan (2006) by Japan Meteorological Agency. Numerals on the right show MSLP (hPa), and left ones indicate the corresponding time (JST). Tornado occurrence points (Nichinan, Hyuuga and Nobeoka) are marked.

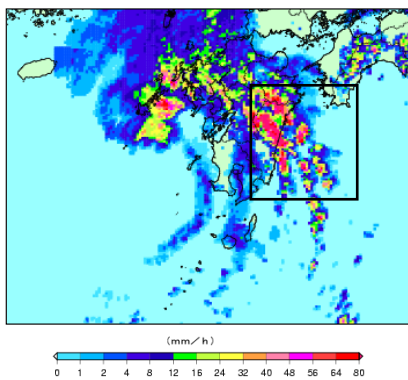


Fig. 2. Precipitation intensity distribution estimated from radar observation at 1400 JST.

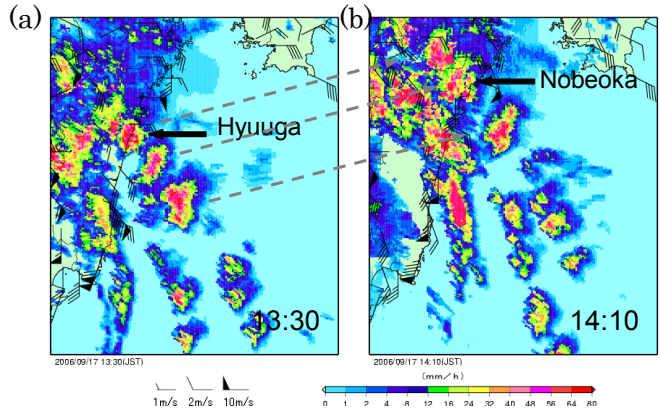


Fig. 3. Same as Fig. 2, but for the rectangle framed area in Fig. 2 (a) at 1330 JST and (b) at 1410 JST.

### 3. Numerical model

The numerical model used in this study is the fully compressible nonhydrostatic model developed by Japan Meteorological Agency (JMANHM; Saito et al. 2006). We employed the bulk-type cloud microphysics scheme with six water species (water vapor, cloud water, rain, cloud ice, snow and graupel) and the turbulent closure scheme that predicts the turbulent kinetic energy. As to the surface boundary condition, bulk exchange coefficients of surface fluxes are determined from the formula by Kondo (1975) over the sea and they are based on Monin and Obukhov's similarity law over the land, depending on the roughness and temperature. To conduct the high-resolution model integration, four telescoping one-way nested grids (Horizontal grid spacing 5 km; NHM5km, 1km; NHM1km, 250 m; NHM250m; 50 m; NHM50 m) were used (Fig. 4a). The vertical coordinate is terrain-following and contains 50 levels with variable grid intervals of  $\Delta z = 40$  m near the surface to 904 m at the top (NHM1km and NHM250m), and 90 levels with  $\Delta z = 40$  m to 304 m (NHM50m). The initial and boundary conditions of NHM5km are provided from the operational regional analysis of JMA. The model domains are shown in Fig. 4b.

### 4. Numerically simulated environmental fields around the rainband

NHM1km successfully reproduced two adjacent rainbands about 300 km away from the typhoon center in the right-front quadrant of translating Shanshan except for about 20 min delay of the precipitation pattern and the typhoon movement (Fig. 5).

The distribution of storm-relative helicity (SREH) shows the large value ( $> 750 \text{ m}^2 \text{s}^{-2}$ ) around the outer rainband (Fig. 6b), which is assumed to correspond to the rainband including the tornado-producing convective cells shown by the radar image (Fig. 3). The wind hodograph around this rainband shows that the strong vertical shear with veering existed below 2 km AGL (Fig. 7).

In the meanwhile, the value of convective available potential energy (CAPE) is about  $1200 \text{ J kg}^{-1}$  around this rainband, which is lower than that of the southern area ( $\sim 2000 \text{ J kg}^{-1}$ ) (Fig. 6c). Though this value is significantly larger than the average CAPE value of the hurricane-tornado environment (e.g.,  $253 \text{ J kg}^{-1}$ ; McCual 1991), it is smaller than that of typical supercell environments over the Great Plains ( $\sim 2500 \text{ J kg}^{-1}$ ).

Therefore, the environmental field around which the tornado occurred was characterized by modest CAPE and strong low-level wind shear with veering. The low-level vertical wind shear is a crucial factor for the occurrence of a tornado. This result is consistent with the previous statistical studies about hurricane-associated tornadoes (eg., McCual 1991).

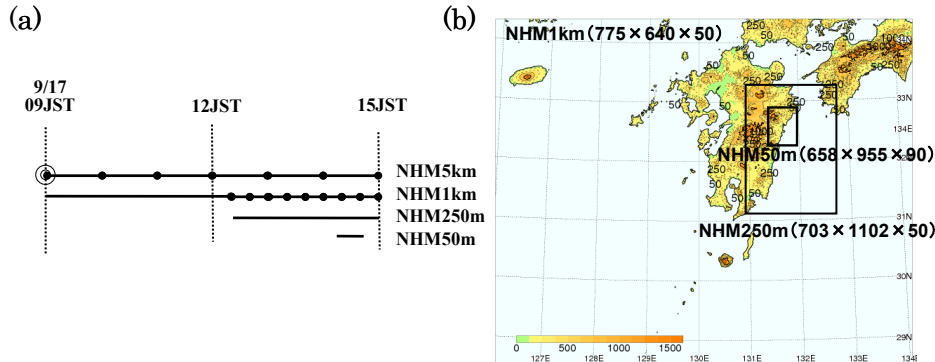


Fig. 4. (a) Nesting procedures of the experiments. (b) Model domains of NHM1km, NHM250m and NHM50m. Numerals show the number of grids on each direction ( $x \times y \times z$ ).

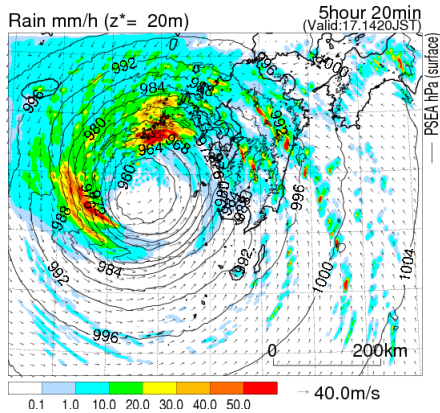


Fig. 5. Distribution of precipitation intensity numerically simulated by NHM1km at 1420 JST.

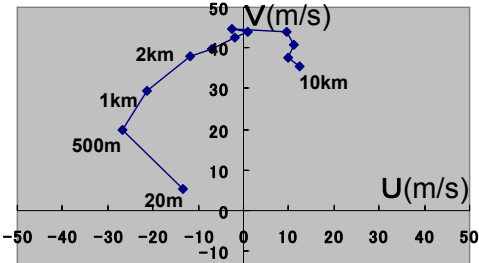


Fig. 7. Winds hodograph at Nobeoka at 1420 JST from the simulation results of NHM1km. Numerals indicate heights. Square-shaped markers are shown with a 1 km interval from 1 to 10 km height.

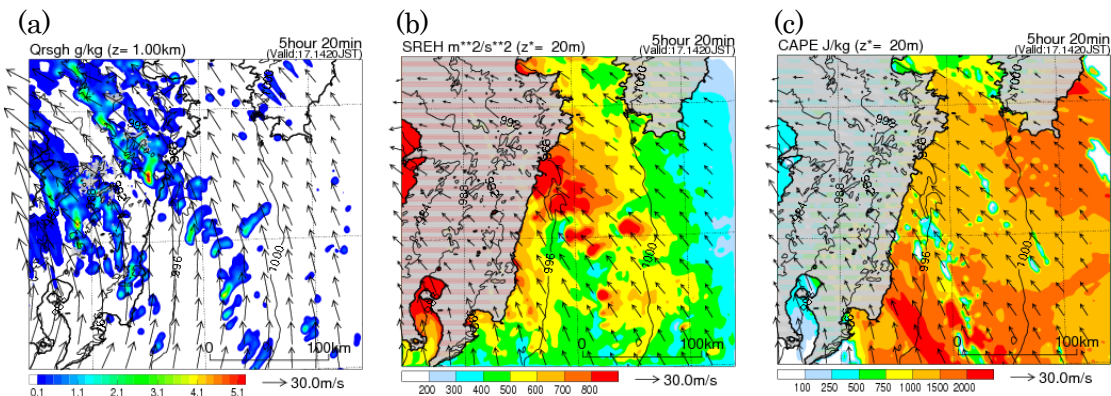


Fig. 6. Distribution of (a) hydrometeors (cloud water, cloud ice, rainwater, snow and graupel) at a height of 1 km, (b) SREH ( $m^2 s^{-2}$ ) and (c) CAPE ( $J \text{Kg}^{-1}$ ) at 1420 JST calculated from the simulation results of the NHM1km. Vectors denote simulated winds (a) at a height of 1 km and (b) - (c) at 20 m AGL.

## 5. Mini-supercell structure numerically simulated by the NHM250m

Figure 8a presents the simulated rainband at 1420 JST by the NHM250m. The outer rainband consists of a number of isolated active convective cells as observed by radar (Figs. 3a and 3b). Some convective cells exhibited characteristics similar to typical supercell storms, such as the hook pattern and bounded weak region of hydrometeors at the southern tip of them (Fig. 8b).

The vertical and horizontal scale is smaller than that of the typical supercell storm over the Great Plains of the United States (Figs. 9a and 9b). These features are identical to the mini-supercell as indicated in many previous studies (eg., Suzuki et al. 2000). The maximum vertical vorticity reached about  $7 \times 10^{-2} \text{ s}^{-1}$  and upward motion is more than  $30 \text{ m s}^{-1}$  around 1 km and 3 km above AGL.

Another noteworthy feature is that the gust font near the surface boundary is distinguishable by the wind field and vertical vor-

ticity (Fig. 10b), however, the horizontal gradient of temperature across it is weak (Fig. 10a). Since the storm was moving north-northwestward at a relatively high speed ( $25 \text{ m s}^{-1}$ ), the storm-relative flow around the forward flank gust front was toward the mesocyclone.

Time evolution of this storm is shown in Fig. 11. The vertical vorticity amplified from the lower level on the gust front in the eastern side of the preexisting mesovortex which was decaying. The maximum vertical vorticity amplified rapidly from 1410 JST and attained  $7 \times 10^{-2} \text{ s}^{-1}$  at about 1 and 3 km AGL at 1420 JST. The region with vertical vorticity greater than  $1.0 \times 10^{-2} \text{ s}^{-1}$  was always confined to the levels below 5 km AGL. As the supercell storm approached the land, it started to decay at the upper level and tilt northwestward. However, it is noteworthy that the vertical vorticity and upward motion at lower level (less than 1000 m AGL) intensified significantly. This storm passed over Nobeoka city around 1430 JST.

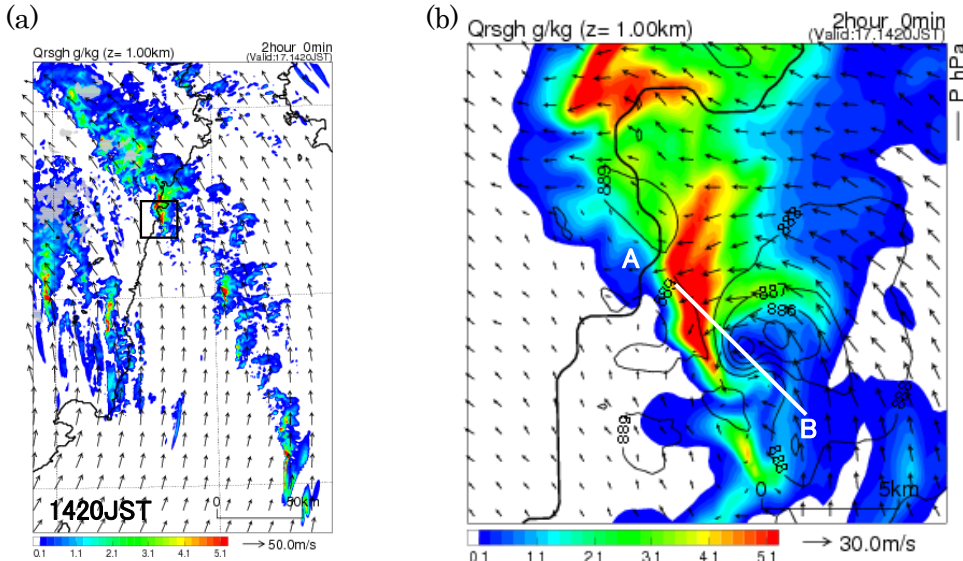


Fig. 8. (a) Horizontal distribution of hydrometeors and wind vectors at a height of 1 km by NHM250m. (b) Enlarged illustration of the square box in Fig. 8a. Contour lines denote the pressure with 1 hPa interval. Arrows show the storm-relative wind.

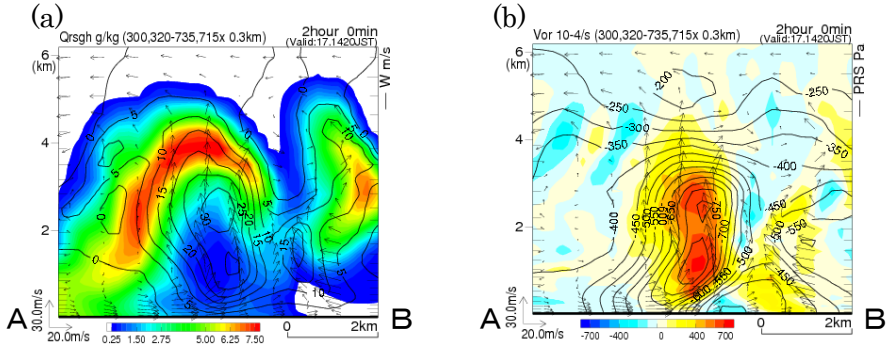


Fig. 9. (a) Vertical cross section along the line in Fig. 8b. Contour lines denote vertical motion with  $5 \text{ m s}^{-1}$  interval. (b) Same as (a), but for vertical vorticity. Contour lines denote pressure deviation with a 50 Pa interval.

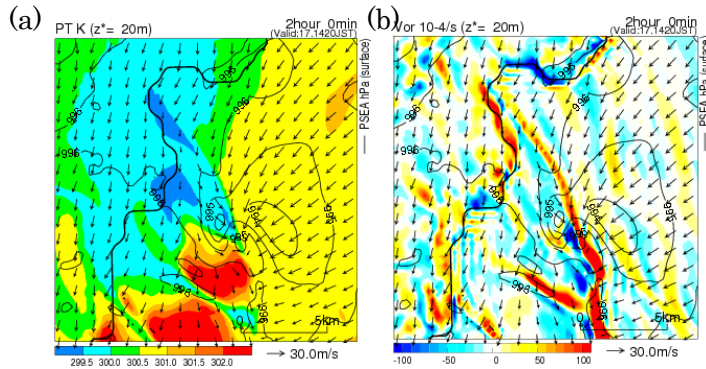


Fig. 10. Same as Fig. 8b but for (a) potential temperature and (b) vertical vorticity with wind arrows and pressure contours at a height of 20 m AGL.

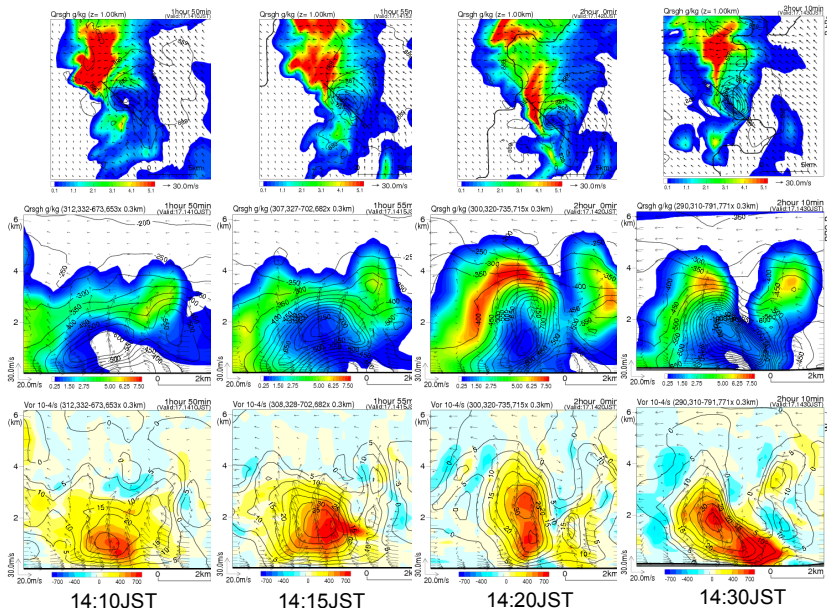


Fig. 11. Time evolution of the simulated supercell storm (1410, 1415, 1420 and 1430 JST). Upper panels show the hydrometeors superposed by pressure with contours (interval: 1 hPa). Middle panels illustrate the vertical cross section along the line in the upper panel. Contours indicate the pressure deviation with a 50 Pa interval. Lower panels are vertical cross section of vertical vorticity along the line in the upper panel superposed by the vertical motion with contours ( $5 \text{ m s}^{-1}$ ).

## 6. Tornado structure numerically simulated by the NHM50m

Figures 12a and 12b show the successfully simulated tornado spawned by the mini-supercell storm noted above. Note that this simulation includes full-physics processes. Therefore, it is unlike the other previous studies employing free-slip and non-topography surface condition.

Obviously, it is difficult to say that this is simulating the observed Nobeoka tornado itself. However, this simulation is assumed to be able to reproduce the representative type of storms that would actually occur on this environmental field.

The tornado was generated on the shore about 2 km southeast from the mesocyclo center determined from the vorticity field at a height of 1 km. The tornado was generated on the rear flank gust front and moved with the rapid translation speed of about  $90 \text{ km h}^{-1}$  toward Nobeoka city. The vertical vorticity reached  $0.7 \text{ s}^{-1}$  and surface pressure drop was about 12 hPa. The diameter of the vortex near the surface is about 500 m. The tornado exhibited the asymmetric structure with strong winds of about  $50 \text{ m s}^{-1}$  only on the right side and tilted northwestward vertically.

Further analytical and numerical studies are

currently underway to investigate the evolution of the mini-supercell storm and the tornadogenesis process.

### Acknowledgments

The author would like to thank T. Kato, S. Hayashi and N. Seino of the MRI/JMA for their support to conduct the numerical simulation.

### REFERENCES

- McCaull, E. W., Jr., 1991: Buoyancy and shear characteristics of Hurricane-tornado environments. *Mon. Wea. Rev.*, 119, 1954-1978.
- Miyazaki District Meteorological Observatory, 2006: On the gust caused by tornado in Miyazaki prefecture associated with Typhoon Shanshan (2006) on 17 September 2006. Meteorological survey report on the natural disaster., 52pp (in Japanese).
- Saito, K., T. Fujita, Y. Yamada, J. Ishida, Y. Kumagai, K. Aranami, S. Ohmori, R. Nagasawa, S. Kumagai, C. Muroi, T. Kato, H. Eito, and Y. Yamazaki, 2006: The operational JMA nonhydrostatic mesoscale model. *Mon. Wea. Rev.*, 134, 1266-1298.
- Suzuki, O., H. Niino, H. Ohno, and H. Nirasawa, 2000: Tornado-producing mini supercells associated with Typhoon 9019. *Mon. Wea. Rev.*, 128, 1868-1882.

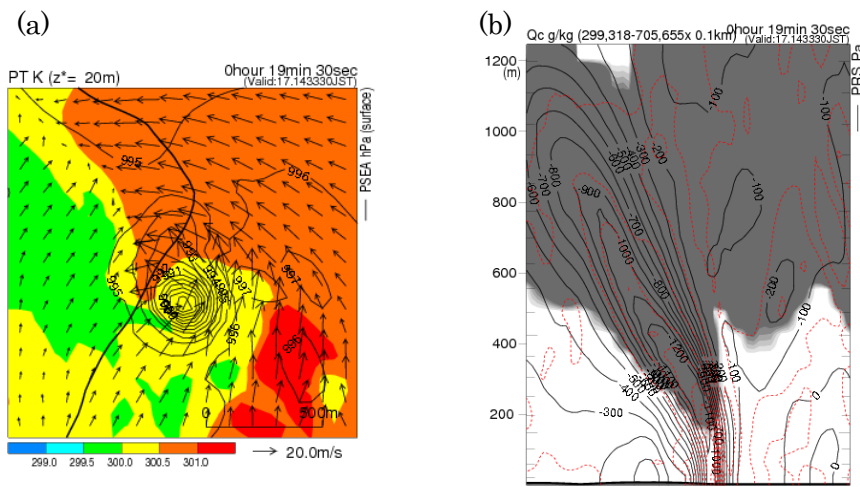


Fig. 12. Simulated tornado structure by NHM50m. (a) Potential temperature with the wind vectors at 20 m AGL. Contour lines denote the surface pressure with 1 hPa interval. (b) Vertical cross section of cloud water along the line in (a). Contour lines denote pressure deviation with a 100 Pa interval, and red ones are vertical vorticity with  $0.1 \text{ s}^{-1}$  interval.